REVIEW ARTICLE   OPEN

Chemical and electrochemical conditions within stress corrosion and corrosion fatigue cracks

Leslie G. Bland[1] and Jenifer S. (Warner) Locke[1]

In the area of environment assisted cracking, literature aimed at understanding the chemical and electrochemical conditions at/ near the crack tip establishes that the crack tip is occluded and not well represented by bulk conditions. A review of the relevant literature, both modeling and experimental, is presented here and shows that crack tip conditions are determined by the balance between high metal ion concentrations resulting from crack tip anodic reactions and subsequent hydrolysis, mass transport (including ion migration, diffusion, and advection), and electrochemical polarization of the bold surface, which determines the extent of anodic and cathodic reactions occurring in the crack environment. Under both freely corroding conditions and anodic polarizations, the crack tip pH decreases with increasing polarization above the freely corroding condition, most often leading to a very acidic crack environment. Under sufficient cathodic polarization, the crack tip pH increases. Because of high-anion and -cation concentrations in the crack environment, an IR drop down the crack exists, leaving the crack tip relatively unpolarizable. Ion migration enhances the occluded nature of the crack tip by supplying anions from the bulk solution to maintain electroneutrality at the crack tip. Diffusion to counteract this concentration gradient is minimal and only plays a role in crack tip conditions at very small crack lengths. When cyclic loading conditions are encountered, the occluded nature of the crack tip can be counteracted by advection; although, the role decreases with decreasing f and increasing R, essentially as corrosion fatigue conditions approach those of stress corrosion cracking.

INTRODUCTION

Structural alloys must withstand both demanding mechanical loads and corrosive environmental conditions when utilized in many applications. Consequently, these materials can be susceptible to premature failure by environment assisted cracking (EAC) when the loading and environmental conditions are sufficiently aggressive. The influence of EAC on the performance and life of structural alloys can be seen in many applications such as oil and gas, nuclear power, nuclear waste storage, and aerospace. For example, several reviews of aircraft structural failures and teardown inspections concluded that fatigue and corrosion dominate aerospace component failures[1,2] with 78% of the corrosion damage sites identified during teardown having initiated fatigue cracks.[2] In addition, the United States Nuclear Regulatory Committee (NRC) released a report in 2014 concluding that one of two top priority needs is understanding stress corrosion cracking (SCC) of spent nuclear fuel storage canisters.[3] These specific findings, as well as similar ones in other industries, demonstrate the importance of quantifying and understanding the synergistic deleterious effects of mechanical loads and sufficiently corrosive environments at the mechanism level.

Although the mechanism by which EAC occurs, anodic dissolution vs. film rupture vs. hydrogen enhanced assisted cracking vs. adsorption-induced dislocation emission, is still debated in structural alloys, particularly for some material system and environment combinations, two things are generally accepted: (1) the chemical and electrochemical conditions of the bulk environment are not maintained down the crack, particularly at the tip, and (2) it is the stress state and chemical/ electrochemical conditions local to the crack tip that control EAC, both for static and monotonically increasing loads, as in stress corrosion cracking (SCC), and cyclic loads, as in corrosion fatigue (CF). This statement is true regardless of the alloy/ environment combination when EAC susceptibility exists. While the stress state ahead of a crack tip is well established, the chemical and electrochemical conditions within the crack have not been well defined, which greatly contributes to the lack of agreement on the mechanism controlling EAC. (Although, It is established that certain conditions sustain crack growth while others deter it; as will be described herein).

Several mathematical based models exist to estimate crack tip chemical and electrochemical conditions,[4–10] but a large majority of these models were developed for nickel and steel alloys. Experimental attempts have been made to measure EAC crack tip chemistry and electrochemistry.[5,8,11–26] While no unified experimental methodology has been utilized and the limited work has been on various metal alloy/environment combinations, experimental evidence supports the theory that crack tip conditions are occluded and not well represented by the bulk environment. Because directly measuring crack chemical and electrochemical conditions is rarely performed given the difficulties in probing and/or extracting electrolyte from the near tip region, a real limitation in advancing the mechanism-based models for EAC and utilizing them for prediction is the availability of experimental input parameters.

[1]Department of Materials Science and Engineering, Fontana Corrosion Center, The Ohio State University, 546 MacQuigg Labs, 105 W Woodruff Ave, Columbus, OH 43210, USA
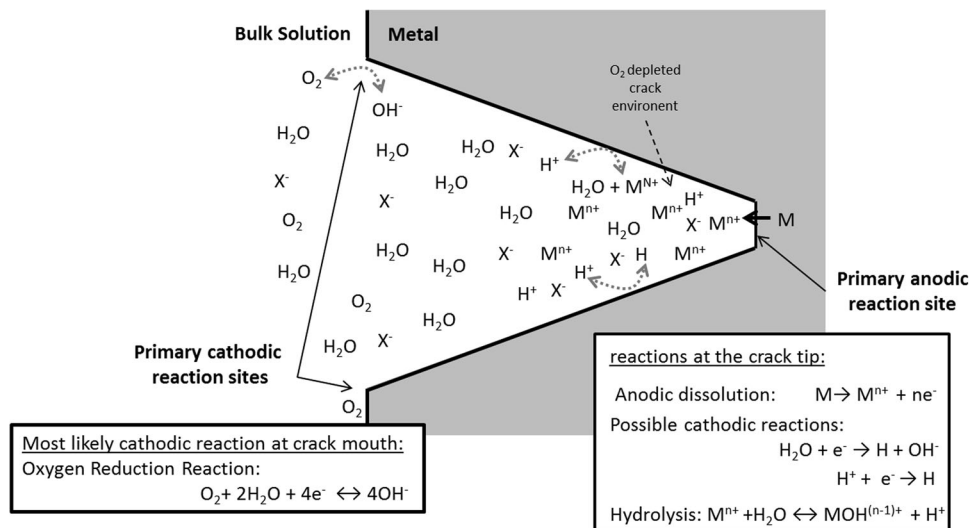Correspondence: Jenifer S. (Warner) Locke (Locke.121@osu.edu)

Fig. 1 Schematic of an EAC crack with relevant chemical and electrochemical reactions and reaction sites shown. Chemical species are shown to schematically represent all factors discussed herein that can create an occluded environment at the crack tip that is depleted in O_2 and concentrated in cations and anions

Several review papers on crack tip chemistry and electrochemistry in either SCC, CF, or EAC in general already exist.[27–30] The most recent and in-depth review was written by Turnbull in 2001 and focused primarily on modeling.[28] Another short introductory and high level review was written by Turnbull in 2013,[29] but mainly presents a description of the present state of understanding and what is required to advance knowledge of crack chemistry and electrochemistry. Other reviews focus on experiment and modeling, but either present only pH and electrochemical potential (E) information[27] and/or only focus on a singular alloy system and environment combination.[30] This paper aims to compliment these reviews by summarizing what is known to date about crack tip chemical and electrochemical conditions.

CHEMICAL/ELECTROCHEMICAL REACTIONS SUPPORTING EAC

Figure 1 provides an overall schematic describing the chemical and electrochemical conditions for EAC. In general, it is expected that the area nearest to the crack tip primarily supports anodic reaction kinetics while the bold surface and crack walls nearest the crack mouth primarily support cathodic reaction kinetics. The assumption that anodic reactions occur predominately at/near the crack tip is supported by the fact that the crack is predicted to quickly become oxygen depleted in comparison to the bulk environment.[28, 31, 32] In typical aqueous electrolytes, the primary cathodic reaction is the oxygen reduction reaction (ORR), which may initially occur anywhere, but reactions along the crack walls will quickly consume and deplete O_2 within the crack. Due to the constrained geometry of a crack and limited crack opening displacements, diffusion of O_2 down the crack after depletion is limited, leading to an O_2 depleted crack environment. The major consequence of this O_2 depletion is to produce a corrosion potential at the crack tip that is more negative than that at the crack mouth/bold surface; and as such, the crack tip is anodically polarized under freely corroding conditions causing a separation of anode and cathode where anodic reactions primarily occur at the crack tip.

The anodic reactions occurring at/near the crack tip are assumed to be primarily anodic dissolution, specifically dissolution of the major element. As pure identification of anodic and cathodic reactions in a crack is not possible experimentally, only measurement of species produced by these reactions, such as the concentration of metal ions from anodic dissolution, can be used to imply whether a specific reaction is occurring. Cooper et al.[15, 16, 33] directly probed SCC crack tip chemistry of AA7050, an Al–Zn–Mg–Cu alloy, and showed that the crack tip became concentrated in Al^{3+} for SCC susceptible tempers. Levels of 1.5–3.5 M Al^{3+} were measured in a bulk solution of 0.5 M Na_2CrO_4 + 0.05 M NaCl. Slightly elevated concentrations of Mg^{2+} and Zn^{2+} were also found. Nguyen et al. also measured elevated concentrations of Al^{3+} under freely corroding and anodic polarizations in three different electrolytes (1 M NaCl: 0.25–0.4 M, 1 M Na_2SO_4: 0.1–0.2 M, and 1 M $NaNO_3$: 0.05–0.1 M). A SCC study on 70:30 Brass in ammonium hydroxide found elevated concentrations of Cu and Zn ions in the crack environment,[24] while another SCC study of various steels in 3.5% NaCl found high Fe and Mn ions in the crack electrolyte.[21]

Due to the high metal ion concentrations in growing EAC cracks, metal cation hydrolysis can result within the near crack tip environment. Figure 1 shows a generic metal ion hydrolysis reaction, and it can be readily seen that hydrolysis can have a large impact on the pH within a crack, as will be discussed later. Directly measuring metal cation hydrolysis near the crack tip is not possible, but the low pH values, to be discussed in a subsequent section, confirm it is occurring. In addition, all modeling efforts take metal cation hydrolysis into account and confirm its occurrence.

Consideration and treatment of any internal crack cathodic reactions is complicated. In general, most models neglect cathodic reactions occurring in the crack environment. Turnbull and co-authors establish the importance of neglected cathodic reactions within the crack environment under freely corroding conditions as well as cathodic polarizations.[4, 8, 20, 28] As will be expounded upon in the pH discussion, increasing the amount of cathodic reactions, specifically reduction of H^+, occurring in the crack environment can result in a more neutral pH. This becomes increasingly important under cathodic polarizations. Additionally, any H produced near the crack tip via cathodic reactions that absorbs into the metal may accelerate dissolution, as has been found for steels.[34] For the hydrogen environment assisted cracking (HEAC) mechanism,[35–47] the occurrence of the cathodic H^+ reduction near the crack tip is critically important to EAC as it is H absorbed after cathodic reduction of H^+ that is proposed to embrittle metals leading to EAC.

CRACK POTENTIAL AND PH

Research has shown that crack tip potential (E_{tip}) and pH deviate from that on the bold surface.[4, 5, 8, 15, 16, 19, 20, 23, 25, 26, 33] Figure 2 is a schematic showing expected E_{tip} and pH conditions for an Al alloy that has a freely corroding potential near −775 mV_{SCE} and a level of IR drop similar to that measured by Cooper and Kelly.[15–17, 33] While Fig. 2 was drawn to replicate an Al alloy, it is applicable for any alloy when the curve is shifted such that the pH independent potential is at a level indicative of the freely corroding potential with compensation for the appropriate amount of IR drop. Experimental and modeling verifications and explanations for this schematic are described in the following section.

Potential

Under freely corroding conditions, E_{tip} differs from the potential of the bold surface due to O_2 concentration differences and an IR drop caused by the high anodic current and ionic concentrations at the crack tip (both metal ion from dissolution and anions from mass transport considerations to be discussed later). For SCC of AA7050 around the T6 temper immersed in 0.5 M Na_2CrO_4 + 0.05 M NaCl, a measured potential difference between the tip and bold surface (ΔE) of ~ 125 mV was found.[16] Additionally, it was observed that the potential gradient was ~ 1 V/cm when measuring E as a function of distance from the crack tip, allowing the authors to concluded that a majority of ΔE is isolated to within 3 mm of the crack tip.[16, 17] Turnbull and Ferris modeled the ΔE for CF of BS 4360 steel grade 50D immersed in ASTM artificial seawater.[4] For an applied potential at/near OCP (~ −800 mV_{SCE}), an ~ 20 mV ΔE was predicted. Scott et al.[25] also studied CF of BS 4360 steel grade 50D immersed in seawater and found a ΔE of 90 mV. En-Hou and Wei[5] modeled and experimentally found a ΔE of ~ 125 mV for CF of a ZG20SiMn low carbon steel immersed in fresh water. While the above described literature results show a large variation in the magnitude of ΔE, all support the fact that the bold surface potential is not maintained at the crack tip.
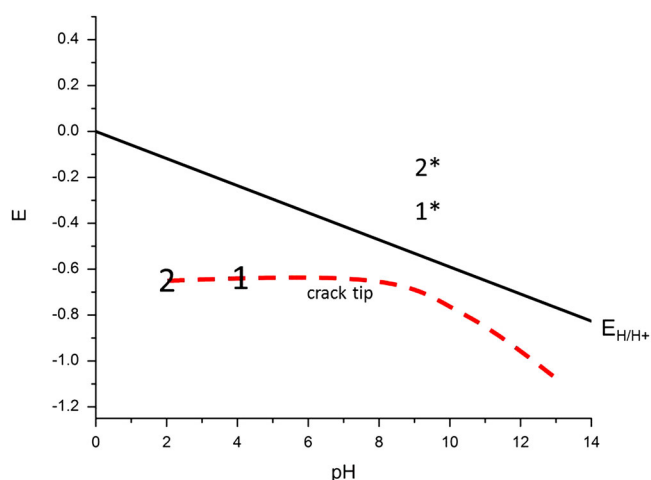

Fig. 2 Schematic illustrating the expected crack tip conditions (*red dashed line*) for an Al alloy. Potential is vs. the SHE electrode. The *black solid line* represents the reversible hydrogen evolution reaction The numbers represent experimental results reported by Cooper and Kelly[16] for an SCC crack of 7050 in the near T6 temper when immersed in 0.5 M Na_2CrO_4 + 0.05 M NaCl. Numbers with a * are for bulk conditions and without are for crack tip conditions. The (1) is for measurements taken when applying the open circuit potential and (2) is when an ~ 200 mV anodic polarization is applied. Note that the slope in the crack tip curve at basic pH is truly schematic as no research was found in the literature presenting crack E and pH measurements for a similar Al alloy under cathodic polarization. The slope in the cathodic polarization region of the curve is estimated based on pH levels measured by Nguyen et al.[49]

Limited research also establishes that E_{tip} is relatively unpolarizable as a function of bulk solution changes (i.e., pH, O_2 concentration, electrolyte composition, and so on) when other factors controlling mass transport remain constant. For a 3% NiCrMoV steel immersed in simulated steam condensate at 90 °C, modification of the bulk pH and Cl- concentration had little effect on E_{tip}.[26] In addition, this same study found that while the bold surface corrosion potential increased with increasing bulk O_2 concentration from near 0.1 ppb to over 1000 ppb, the crack tip potential remained relatively constant with a maximum change being ~ 90 mV.[26] This means that while the potential drop, ΔE, will change as a function of bulk O_2 concentration; this is only due to changes in the bold surface corrosion potential. Modeling efforts have probed this by varying the rates of oxygen reduction and found that the primary effect is on the potential drop with minor influences on crack tip conditions; although uncertainty in appropriate oxygen reduction kinetics made this analysis difficult.[8]

Several researchers have modeled and/or experimentally determined E_{tip} and/or ΔE as a function of anodic and cathodic polarization and established that the crack tip is not polarizable, meaning ΔE will become more severe as polarization increases. For CF of the BS 4360 steel grade 50D immersed in ASTM artificial seawater studied by Turnbull and Ferris,[4, 8] ΔE increased from ~ 20 mV (E is −800 mV_{SCE}, which is approximately OCP)[4] to ~ 146 mV when −500 mV_{SCE} was applied to the bold surface[8]. Cathodic polarizations were also examined by Turnbull and Ferris with similar findings; ΔE increased from ~ 20 mV to as much as ~ 215 mV with an applied potential of −1200 mV_{SCE}.[4] For various anodic polarizations of AA7050 near the T6 temper, E_{tip} remained at ~ −730 mV_{SCE}, similar to that observed when applying OCP (~ −600 mV_{SCE}), for all anodic polarization levels examined (up to an applied potential of −300 mV_{SCE}).[16] This means that even with a strong anodic polarization of 300 mV, the crack tip remained unpolarized and ΔE increased from −125 mV at OCP to −425 mV at −300 mV_{SCE}. For cathodic polarizations, E_{tip} was unaffected for polarizations of less than 100 mV (applied potentials between −600 and −700 mV_{SCE}).[16] For applied potentials between −700 and −800 mV_{SCE}, the crack tip was polarized to at or near the applied potential.[16] For the singular potential examined below −750 mV_{SCE}, the crack tip potential was slightly more cathodic.[16] A study on 3% NiCrMoV steel immersed in simulated steam condensate at 90 °C, reported that the crack tip had limited polarization under significantly anodic potentials (up to 0.0 V_{SCE}) with the crack tip reaching a limiting value of −0.61 mV_{SCE}.[26]

It is important to note that crack depth does play a role. The above analysis typically assumes a long crack. Modeling and limited experimental efforts confirm that ΔE in small in very short cracks (~ 0.2 cm and below).[4, 8]

pH

The pH at/near the crack tip is established by the balance between the metal ion concentration from crack tip dissolution and hydrolysis, mass transport, and the polarization of the crack (anodically or cathodically, which determines the extent of anodic and cathodic reactions occurring in the crack environment). As such, it is generally true that the bulk pH does not significantly influence the crack tip pH unless there is significant convective mixing, as will be discussed in the mass transport section. Crack tip pH when the impact of advection is minimal will be discussed here.

As a result of the high metal ion concentration at/near the crack tip and subsequent hydrolysis, a crack tip under freely corroding conditions becomes acidic, as can be readily seen through the generic hydrolysis reaction shown in Fig. 1. In fact, stable pH values can be achieved in the crack tip environment once equilibrium between H^+ and the metal ion concentration is attained, as would be suggested by speciation diagrams.

Essentially, it is the balance between metal ion concentration and hydrolysis that buffers the pH in an occluded crack environment. The acidic nature of the crack tip has been experimentally confirmed by several researchers on both Al- and Fe-based alloys. Nguyen et al.[48] measured the developing pH at the tip of SCC cracks in AA7075-T651 exposed to 1 M NaCl, 1 M NaNO$_3$, and 1 M Na$_2$SO$_4$. When the potential of the external surface was maintained at OCP, the pH at the tip of the crack was 3.4 for both the NaCl and Na$_2$SO$_4$ electrolytes. Because of the formation of ammonia and the absence of a crack tip anion to react with Al^{3+} in nitrate solutions,[48] the pH in NaNO$_3$ was 9.1. It is important to note that this pH is lower than that found under cathodic polarization and anodic polarization in NaNO$_3$, which is consistent with expectations. The effect of hydrolysis on crack tip pH was noted in a study on various types of alloy steels exposed to 3.5% NaCl, where the bulk solution pH was 6 and the pH near the crack tip for all steel alloys investigated was ~ 3.7.[21] Additionally, for SCC tests on AISI 4340 steel exposed to 3.5% NaCl with various bulk solution pH's between 1 and 10, the crack tip pH was independent of the bulk solution pH and near 3.7 in all cases.[21] This agrees with a study on CF of X70 pipeline steel in an electrolyte of near neutral pH containing CaCl$_2$, KCl, MgSO$_4$, and NaHCO$_3$ where in situ measurements established a pH of ~ 4 within the crack.[49] Smith et al.[13] also showed that the pH within a crack for 4340 steel immersed in 0.6 M NaCl with a bulk pH of 5.6 consistently remained between 3.5 and 3.9.

Furthermore, Smith showed that a crack tip pH of 3.5–3.9 was unaffected by changes in the bulk pH by altering the bulk pH between 2 and 10 through additions of HCl and NaOH. In all, experimental findings on both Al and Fe-based alloys agree with model predictions by establishing that the balance between metal ion concentration and hydrolysis controls crack tip pH and establishes an acidic crack tip environment under freely corroding conditions.

It is important to note that Turnbull and co-authors have shown, through modeling and experimentation that an appreciably acidic crack tip pH under freely corroding conditions does not develop for a low alloy steel in seawater[4, 8, 20, 28] as might be assumed based on the previous discussion. This is attributed to a limit in acidification based upon the reversibility of the Fe electrode, which facilitates increased cathodic reaction kinetics, specifically reduction of H$^+$, in the crack counteracting hydrolysis.[4, 8, 20, 28] Although Turnbull and Ferris[8] did observe a lowering in the crack tip pH with increasing anodic polarization, consistent with the trends and predictions described below, the lowest pH observed was 7.8 at an applied anodic potential of −500 mV$_{SCE}$ (OCP is ~ −680 mV$_{SCE}$ at pH 8[20] and ~ −800 mV$_{SCE}$ at pH 10.2[4]).[8]

Both Nguyen et al. and Cooper et al. concluded that crack tip pH is controlled by the Al^{3+} concentration ([Al^{3+}]) and subsequent metal ion hydrolysis.[16, 33, 48] Cooper et al.[33] went even further to state that anything that alters the rate of metal ion production at the crack tip will also alter crack tip pH. As such, anodic polarization of the bold surface should serve to increase crack tip anodic reaction kinetics, and therefore increase the crack tip [Al^{3+}] and consequently drive an increasingly acidic crack tip. For SCC of AA7075-T651 immersed in 1 M NaCl and 1 M Na$_2$SO$_4$, Nguyen et al.[48] directly observed that increases in the level of applied anodic polarization increased crack tip [Al^{3+}] and crack tip acidity. Cooper et al. measured crack tip pH during SCC of AA7050 aged to near the T6 temper in 0.5 M Na$_2$CrO$_4$ + 0.05 M NaCl with a bulk pH of 9.2 and observed an increasingly acidic crack tip pH with increasing anodic polarization.[16, 33] Specifically, the crack tip pH was 4 when polarized to −0.645 V$_{SCE}$ and 2.5 when polarized to −0.445 V$_{SCE}$.[16] Cooper et al., in collaboration with Young et al., correlated increases in applied anodic polarization to corresponding shifts in (1) crack tip pH from bulk like (pH of 8.5–9) to very acidic (pH of 4–2.5), (2) [Al^{3+}] from nominal concentrations to as high as 1.5–3.5 M, and (3) changes in crack growth rates (da/dt)

from incubation-type slow crack growth (as low as 5.5×10^{-7} mm/s) to active fast crack growth (as high as 1×10^{-4} mm/s).[15, 16, 33, 50, 51] Nguyen also showed increases in stage II da/dt with increasing anodic polarization and correlated these changes to acidified pH and higher [Al^{3+}].[48]

The work by these authors directly supports the well agreed upon theory that high metal ion concentrations developing due to anode (crack tip) to cathode (crack mouth/bold surface) separation drive an acidic crack tip that results in EAC susceptible conditions and fast crack growth, and anything that increases crack tip metal ion concentrations will act to decrease crack tip pH (to a limit defined by the balance between hydrolysis and metal ion concentration) and increase crack growth rates.[16, 33, 48]

Just as anodic polarization acts to increase crack tip dissolution, driving a decrease in crack tip pH and increase in crack growth kinetics, cathodic polarization of the bold surface will (1) increase the cathodic reaction kinetics within the crack (thereby increasing crack [OH$^-$] and/or consuming H$^+$), (2) decrease the rates of crack tip anodic dissolution, and subsequently, (3) reduce crack tip metal ion concentrations; therefore yielding less acidic crack tip environments. Nguyen et al. observed basic crack tips for SCC of 7075-T651 under cathodic polarization when immersed in 1 M NaCl (measured pH of 9.5 at −0.758 V$_{SHE}$ and 12 at −1.056 V$_{SHE}$, the OCP is −0.606 V$_{SHE}$), 1 M Na$_2$SO$_4$ (measured pH of 11.5 at −1.163 V$_{SHE}$, the OCP is −0.498 V$_{SHE}$), and 1 M NaNO$_3$ (measured pH of 12.5 at −1.184 V$_{SHE}$, the OCP is −0.400 V$_{SHE}$).[48] It is notable that Nguyen also observed low [Al^{3+}] (0.01 M for both the NaCl and Na$_2$SO$_4$ electrolytes) and relatively low stage II da/dt under these levels of cathodic polarization.[48] Turnbull and co-authors modeled and experimentally probed BS 4360 grade 5OD steel under cathodic polarizations;[4, 20, 28] and in one model prediction for 3.5% NaCl and seawater with and without O$_2$, Mg, or HCO$_3^-$, Turnbull et al. found that pH increased for all bulk environments from a range of 10–11.5 when polarized near OCP (~ −800 mV$_{SCE}$ when pH is 10.2) to a range of 10.8–12.5 when polarized to −1100 mV$_{SCE}$.[4] (The exact pH in these ranges depends on the specific environment). It is important to note that this Turnbull study[4] looked at a range of cathodic polarizations between −800 and −1100 mV$_{SCE}$ and attributed control of the crack tip pH to different buffering reactions depending on the electrolyte composition; but nevertheless the decreased contribution of metal ion hydrolysis because of cathodic polarization allowed for the development of a basic crack tip pH. Experimental results from this same study[4] confirmed increasing pH with increasing cathodic polarization; although the absolute value of pH was slightly different from the model result, which was attributed to crack tip dissolution and hydrolysis creating a slightly lower pH than predicted in the model.[4] Similar work by Turnbull et al.[20] on BS 4360 5OD steel immersed in seawater, showed crack tip pH levels increase from 7.3 to 8.5 at OCP to as basic as 13.0 under a cathodic polarization at −1100 mV$_{SCE}$ (the OCP is ~ 680 mV$_{SCE}$ at pH ~ 8).[20] Turnbull[28] provides an in-depth review of the various models developed to estimate crack tip pH, among other things, particularly under cathodic polarization conditions where crack tip pH is more strongly dependent upon the balance of increasing internal cathodic reactions consuming H$^+$ and crack acidification through metal dissolution and hydrolysis.

MASS TRANSPORT

The main sources of mass transport within a crack are diffusion, ion migration, and advection from convective mixing. It is through the balance of these three that differences between CF and SCC crack tip conditions are understood.

Ion migration

As established previously, high metal ion concentrations can exist near the crack tip. In order to maintain electroneutrality, ion migration of negatively charged ions (i.e., Cl^-, OH^-, and so on) to the crack tip must occur which results in the crack tip becoming concentrated in both cations and anions. For SCC, ion migration can be particularly potent as the material is confined to static loading conditions where advection is precluded.

Several researchers have presented experimental evidence supporting the role of ion migration by showing that crack tip concentrations of Cl^- and other anions present in the bulk solution are elevated above bulk concentrations.[11, 13, 15, 16, 21, 33] For SCC of 7050 in the T651 and T7541 tempers immersed in 0.5 M Na_2CrO_4 + 0.05 NaCl, measured crack tip $[Cl^-]$ concentrations were elevated by approximately an order of magnitude over the bulk in EAC susceptible tempers (400–500 mM near the tip vs. 50 mM in the bulk).[15, 16, 33] Similarly, elevated CrO_4^{2-}. $_4^{2-}$ concentrations were found at the crack tip (2–3 M near the tip vs. 0.5 M in the bulk).[15] In EAC resistant tempers, which have low crack growth rates (da/dt) compared to EAC susceptible tempers, elevated anion concentrations were found as well.[15] However, for the EAC resistant tempers, elevations in anion concentration did not persist as far into the crack wake, and in the case of Cl^-, did not reach as high of concentrations.[15] For sensitized 304L stainless-steel exposed to simulated Boiling Water Reactor water, Peng et al. observed Cl^- and SO_4^{2-} at the crack tip (1.01 p.p.m. Cl^- and 0.50 p.p.m. SO_4^{2-} at/near the crack tip) when no such anions were detected in the bulk environment.[12]

Because the crack tip becomes concentrated in cations associated with metal dissolution, H^+ ions associated with metal hydrolysis, and anions to maintain electroneutrality; bulk electrolyte composition should have a minimal influence on crack tip chemistry. That being said, the existence or absence of a species from the bulk solution will have an effect. For example, the addition of passivating inhibitors such as chromate or molybdate, when present in sufficient quantities, have been found to slow crack growth in EAC[39, 52–54] for various Al alloys. It is outside of the scope of this paper to elaborate on EAC inhibition, but references can be consulted for further information.[39, 52–54] The absolute value of the bulk concentration has a minimal effect as the crack tip becomes concentrated due to ion migration, as driven by crack reactions and the need to maintain electroneutrality.

Advection/convection

Advection (or convective fluid mixing) is due to the overall motion of the fluid into and out of the crack and allows some degree of mixing the crack and bulk electrolyte. For SCC, advection is typically considered negligible as the crack mouth does not experience opening and closing. On the other hand during CF advection occurs through the cyclic loading and unloading that causes displacement of the crack walls, which acts to pump fresh electrolyte from the bulk into the crack. As a result, CF conditions may be less severe than in SCC. Factors that contribute to convective mixing are fatigue loading frequency (f), stress intensity range ($\Delta K = K_{max} - K_{min}$, where K is the stress intensity factor), and stress ratio ($R = K_{min}/K_{max}$, representative of how close K_{mean} is to zero and the crack is to closing—an R of 0 means the crack is closing at K_{min}). Note the contribution of ΔK to advection is predicted to be negligible[4, 8] but ΔK will be discussed here where other CF parameters are pertinent. It is also important to note that crack length plays a role in determining the severity to which these contributing factors alter crack tip chemistry. Modeling estimates confirm that longer cracks have more occluded environments as the role of diffusion to offset advection decreases as crack length increases.
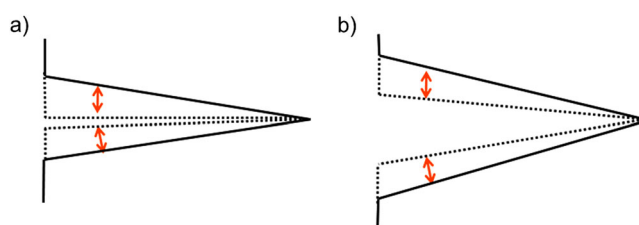

Fig. 3 A schematic for a CF crack with a low R-value **a** high R-value **b** at a constant ΔK. $\Delta K = K_{max} - K_{min}$, and is represented by the orange arrows being similar in magnitude. $R = K_{min}/K_{max}$ and is representative of how close K_{mean} is to 0

f

Because advection occurs due to the overall motion of the crack walls through a load cycle, increasing f allows for an increased contribution of advection. As the f decreases, more time is available for crack tip anodic dissolution, subsequent hydrolysis, ion migration, and diffusion. Therefore, as f decreases, the crack tip becomes more occluded and mixing with the bulk environment plays a diminished role in determining crack tip conditions. It should therefore be noted that approaching a f of zero should yield SCC crack tip conditions. Turnbull and Ferris predict a critical f of ~ 1 Hz below which advection is negligible;[4] but because the amount of time during a load cycle continues to increase with decreasing f, a f effect persists below 1 Hz. Turnbull and Ferris showed that pH changes as f increases from 0.1 to 1 Hz.[4] Increasing f also acts to increase ΔE,[4] which may be due to an increasing contribution of oxygen reduction within a single cycle at the crack mouth.[55]

R

For a constant ΔK, an increasing R yields a crack mouth that is more open during the full loading cycle as shown in Fig. 3, and a higher K_{mean} (and mean stress). This means that the magnitude to which the crack walls flutter is the same, but the mean crack opening changes with R. Because lower R yields a crack that more fully closes, mixing of the bulk and crack tip electrolyte is enhanced through an increasing contribution of advection. Therefore, lower R is expected to have a crack tip chemistry that is less occluded. Although, a lower R also creates a tighter crack, which yields and increased IR drop down the crack; and therefore, an increased ΔE. Higher R allows for a larger volume of crack solution for the same crack wall surface area, which can affect the extent of cathodic reactions occurring within the crack. Turnbull et al.[8] modeled the effect of R on ΔE under freely corroding conditions showing a 30 mV ΔE for a R of 0.1 and 1 mV for 0.8. A similar change in ΔE was seen under cathodic polarization.[4] Turnbull et al.[20] confirmed experimentally that low R produces the greatest ΔE. Turnbull modeled the effect of R on crack chemistry establishing that higher R produces a more occluded crack environment and lower R maintains bulk like chemistry deeper into the crack.[31]

ΔK

For a constant R and crack depth, increasing ΔK yields a crack mouth that is more open (K_{mean} is higher) which can facilitate a greater solution volume to area ratio. As such, IR drop, and therefore ΔE, should decrease with increasing ΔK. Modeling establishes that increasing ΔK from 10 to 40 $MPa\sqrt{m}$ for steel at OCP in seawater produces a decrease in ΔE from ~ 60 mV to ~ 16 mV for a 2 cm long crack.[8] This finding was experimentally confirmed in another Turnbull et al.[20] work. There is no predicted significant influence of ΔK on electrolyte replenishment.

Diffusion

Due to the occluded nature of a crack, diffusion plays a diminished role in determining crack chemistry and electrochemistry as crack length increases. A shorter crack length (a) (i.e., the tip is closer to the bold surface), assuming constant R, ΔK, f, and notch depth, allows for enhanced polarizability and an increased contribution of diffusion from the bulk environment due to the decreased diffusion length. Therefore shorter cracks tend to have lower ΔE and a less occluded environment. Turnbull modeled the contributions of diffusion and advection in controlling crack chemistry during CF and showed that for short crack lengths, below a critical value, diffusion dominates in establishing crack chemistry; while for long crack lengths, above a critical value, ion transport and advection dominate and drive an occluded crack tip environment.[31] Turnbull et al. modeled the effect of crack depth on ΔE for a structural steel in seawater and observed no ΔE under OCP (-690 mV$_{SCE}$) and anodic polarization for very short cracks (2.5×10^{-2} cm). However, for a crack measuring 2 cm in-depth, ΔE was 35 mV at OCP and 80 mV under a 90 mV anodic polarization.[8] For steel in seawater under a cathodic polarization of -1100 mV$_{SCE}$ Turnbull et al.[4] observed a ΔE increase from 0 V for a crack measuring 2.5×10^{-2} cm to ~ 70 mV for a 2 cm long crack. Interestingly, through collaborative efforts examining SCC of 7050 in SCC susceptible and resistance tempers, researchers identified a critical applied transition potential below which diffusion can play a role in reducing development of aggressive crack tip conditions.[16–18, 50, 51] A crack length dependence on this critical transition potential was not examined.

PREVAILING KNOWLEDGE GAPS

While the review above details the knowledge to date on crack chemical and electrochemical conditions some prevailing gaps remain. As stated previously, some of these gaps are a direct consequence of a lack of experimental data to verify and improve modeling efforts. Directly measuring crack solution chemical and electrochemical conditions is rarely performed given the difficulties of probing and/or extracting electrolyte from a growing crack. The earliest attempts[11, 15] utilized EAC specimens that were frozen in liquid nitrogen immediately after testing. After freezing, fracture specimens were broken in half, filter paper or pH paper placed on the fracture surface, and fracture surfaces held back together in order to allow the filter/pH paper to absorb the crack solution upon thawing. The electrolyte collected by the filter paper was then analyzed using capillary electrophoresis. While useful, this approach does not allow one to directly probe the crack electrolyte instantaneously in situ and assumes that the electrolyte at different positions within the crack will not mix when thawing and absorbing into the filter paper. Additionally, no information on electrochemical potential, which is one of the primary variables controlling the environmental driving force for cracking, can be gained. More advanced attempts have utilized holes drilled into fracture mechanics specimens.[12, 14–16, 33] Holes have primarily been drilled into the back-end of the specimen in the fracture plane, but some studies have drilled a series of top down holes to allow for sampling along the crack wake and at different crack depths. When the crack meets a drilled hole a small amount of electrolyte can be withdrawn and analyzed, typically via capillary electrophoresis. These studies have differing limitations; some only sample the crack tip and do not get information along the wake, and most do not measure crack potential. One study that did sample different crack lengths paused cracking and washed the system between growth and sampling events,[12] this clears the occluded environment and may reduce the saturation of ions and severity of pH at the crack tip. The most comprehensive experimental study to date was performed by Cooper and Kelly[15, 16, 33] on SCC of 7050-T6 in sodium chloride solutions. All in all, the most recent experimental work establishes that measuring, monitoring, and changing the crack chemical and electrochemical conditions is possible, and recent advances in micro-electrodes offer improvements. But because the limited experimental attempts utilize different metal alloy/environment combinations and individualized techniques, a holistic knowledge set to fine tune a rigorous model does not exist. This is a major limitation holding back progress in the field, as noted by Turnbull.[29]

When modeling crack chemistry and pH, typically only hydrolysis of the main element (Al or Fe) is taken into account and precipitation of species and plating of metals on the crack is not considered. Experimental efforts have found that other metal cations are present in the crack electrolyte after crack tip metal dissolution; and as such, some of these cations may undergo hydrolysis and affect the crack tip pH. Turnbull et al. included hydrolysis of chromium in their modeling of SCC and CF crack electrochemistry of steels in marine environments.[8, 56] While assumptions on chromium dissolution rates and hydrolysis numerical solutions made exact prediction of crack tip pH difficult, the authors concluded that dissolution and hydrolysis of alloying elements can be important. Indirect evidence of the importance of alloying element hydrolysis in the crack environment has been noted by Crane et al.[57] for Al–Mg alloys where MgCl$_2$ additions to bulk concentrated AlCl$_3$ crack simulated solutions were made to estimate the impact of Mg dissolution and hydrolysis on crack pH for sensitized high-Mg 5xxx Al alloys. It was found that addition of MgCl$_2$ decreased bulk solution pH below 1. Recent theories on the effect of metal cations plating onto fracture surfaces and affecting crack tip pH and crack growth kinetics have been published[58, 59] but cannot be verified as this has not been incorporated into models and is difficult to experimentally detect.

While it is well established that the crack tip becomes heavily concentrated in both cations and anions, the resulting impact of this is not entirely well understood or captured by models. It is known and seen in many SCC and CF experimental studies that supersaturation producing precipitated corrosion products occurs within the crack environment. It is also possible that salt films form on the crack tip and along the wake. Unfortunately, experimental techniques are not capable of determining the existence of an actual salt film as most extracted solutions are small in volume and must be diluted to make a larger solution volume for analysis. As noted by Turnbull, modeling is not yet capable of capturing the effects of concentrated solutions.[28] As such, little is known about changes and effects of solution viscosity, precipitated salt films causing decreased dissolution kinetics, and any dehydration from water molecule complexation. Some work has been done on pit and/or crevices in the areas of understanding salt films and the use of activity gradients instead of concentration gradients. While work on pits and crevices may serve as a start for understanding the highly concentrated crack electrolyte, it will not be discussed here.

SUMMARY OF KNOWLEDGE TO DATE AND CONCLUSIONS

It is well established through modeling and experimentation that the crack tip is occluded and not well represented by bulk conditions. This is due to the fact that diffusion of O$_2$ into a crack is difficult and a growing crack will quickly become O$_2$ depleted, which results in the separation of anode and cathode. As such, the O$_2$ depleted crack tip will become the primary anodic reaction site while the crack mouth will serve as the primary cathodic reaction site. Anodic dissolution occurring primarily at the crack tip can result in high metal ion concentrations leading to hydrolysis, which acidifies the crack tip. The balance between the metal ion concentration and subsequent hydrolysis, mass transport (including ion migration diffusion, and advection), and the polarization of the crack (anodically or cathodically) determines the chemical and electrochemical conditions at the crack tip. Under freely corroding conditions and anodic polarizations, the crack tip is predicted to

become more acidic, while under cathodic polarization the crack tip trends more basic. Because of high-anion and -cation concentrations in the crack environment an IR drop down the crack exists and the crack tip is relatively unpolarizable. This ΔE between the tip and bold surface becomes more extreme in situations that encourage crack tip dissolution (anodic polarization) or a tighter crack (low R). Ion migration contributes to aggressive and occluded crack tip conditions by facilitating migration of anions from the bulk solution as a means of maintaining electroneutrality. Diffusion to counteract this concentration gradient is minimal and only plays a role in establishing crack tip conditions at very small crack lengths. When cyclic loading conditions are encountered, the occluded nature of the crack tip can be counteracted by advection; although, the role of advection decreases with decreasing f and increasing R.

While much is known about crack chemistry and electrochemistry from modeling and experimental efforts, there are still some prevailing knowledge gaps, particularly with respect to understanding and modeling the effects of concentrated small solution volumes. Advancements in experimental techniques to experimentally probe and alter crack chemistry and electrochemistry, an increase in these types of experiments to generate more detailed and controlled experimental data, and collaboration of experimental and modeling efforts would allow for advancements in understanding. Advancement in modeling and characterizing crack chemistry and electrochemistry could benefit various areas, but one notable area in need of this knowledge is verification of the precise mechanism(s) driving EAC. The mechanism driving EAC in aqueous environments is still heavily debated. Papers arguing one of the two leading proposed mechanisms, HEAC and film rupture—anodic dissolution, date back to the 1970s and 1980s. As aqueous EAC occurs via electrochemical and mechanical processes all highly localized near the crack tip, knowledge of crack tip chemical and electrochemical conditions is vital to understanding the mechanism driving EAC. Determination of the mechanism(s) would allow for the creation of life prediction models from first principles and enhance our understanding of EAC crack growth kinetics, the effects of precipitated or deposited surface films and metals, and crack growth inhibition.

Data availability
Data sharing not applicable to this article as no data sets were generated or analyzed during the writing of this review.

AUTHOR CONTRIBUTIONS
L.G.B. and J.S.W.L. equally contributed to this work by conducting literature searches. L.G.B. worked on literature summaries that J.S.W.L. incorporated into the written review.

ADDITIONAL INFORMATION
Competing interests: The authors declare that they have no competing financial interests.

Publisher's note: Springer Nature remains neutral with regard to jurisdictional claims in published maps and institutional affiliations.

REFERENCES
1. Findlay, S. & Harrison, N. Why aircraft fail. *Mater. Today* **5**, 18–25 (2002).
2. Shoales, G. A., Fawaz, S. A. & Walters, M. R. in *ICAF 2009, Bridging the Gap between Theory and Operational Practice* 187–207 (Springer, 2009).
3. Commission, U. S. N. R. C. *Identification and Priorization of the Technical Information Needs Affecting Potential Regulation of Extended Storage and Transportation of Spent Nuclear Fuel*. Report No. ML14043A402. (2014).
4. Turnbull, A. & Ferriss, D. Mathematical modelling of the electrochemistry in corrosion fatigue cracks in structural steel cathodically protected in sea water. *Corros. Sci.* **26**, 601–628 (1986).
5. En-Hou, H. & Wei, K. Chemical and electrochemical conditions within corrosion fatigue cracks. *Corros. Sci.* **35**, 599–610 (1993).
6. Turnbull, A. Modelling of crack chemistry in sensitized stainless steel in boiling water reactor environments. *Corros. Sci.* **39**, 789–805 (1997).
7. Turnbull, A. & Thomas, J. A model of crack electrochemistry for steels in the active state based on mass transport by diffusion and ion migration. *J. Electrochem. Soc.* **129**, 1412–1422 (1982).
8. Turnbull, A. & Ferriss, D. Mathematical modelling of the electrochemistry in corrosion fatigue cracks in steel corroding in marine environments. *Corros. Sci.* **27**, 1323–1350 (1987).
9. Ateya, B. & Pickering, H. On the nature of electrochemical reactions at a crack tip during hydrogen charging of a metal. *J. Electrochem. Soc.* **122**, 1018–1026 (1975).
10. Van der Wekken, C. & Janssen, M. Solute transport in corrosion fatigue cracks. *J. Electrochem. Soc.* **138**, 2891–2896 (1991).
11. Brown, B., Fujii, C. & Dahlberg, E. P. Methods for studying the solution chemistry within stress corrosion cracks. *J. Electrochem. Soc.* **116**, 218–219 (1969).
12. Peng, Q., Li, G. & Shoji, T. The crack tip solution chemistry in sensitized stainless steel in simulated boiling water reactor water studied using a microsampling technique. *J. Nucl. Sci. Technol.* **40**, 397–404 (2003).
13. Smith, J. A., Peterson, M. H. & Brown, B. F. Electrochemical conditions at the tip of an advancing stress corrosion crack in AISI 4340 steel. *CORROSION* **26**, 539–542 (1970).
14. Andresen, P. & Young, L. Crack tip microsampling and growth rate measurements in low-alloy steel in high-temperature water. *Corrosion* **51**, 223–233 (1995).
15. Cooper, K. R. & Kelly, R. G. Using capillary electrophoresis to study the chemical conditions within cracks in aluminum alloys. *J. Chromatogr. A.* **850**, 381–389 (1999).
16. Cooper, K. R. & Kelly, R. G. Crack tip chemistry and electrochemistry of environmental cracks in AA 7050. *Corros. Sci.* **49**, 2636–2662 (2007).
17. Cooper, K. R. *Chemisty and Electrochemsity of Environment-Assisted Cracking of an Al-Zn-Mg- Cu Alloy*. Ph.D. thesis, Univ. Virginia, (2001).
18. Cooper, K. R., Young, L. M., Gangloff, R. P. & Kelly, R. G. The electrode potential dependence of environment-assisted cracking of AA7050. *Mater. Sci. Forum* **331–337**, 1625–1634 (2000).
19. Turnbull, A. Comparison of hydrogen charging of structural steel by crack tip processes and by bulk reactions in the cathodic protection of corrosion fatique cracks. *Scrip. Metal.* **20**, 365–369 (1986).
20. Turnbull, A., Dolphin, A. S. & Rackley, F. A. Experimental determination of the electrochemistry in corrosion fatigue cracks in structural steel in artificial seawater, *CORROSION* **44**, 55–61 (1988).
21. Sandoz, G., Fujii, C. & Brown, B. Solution chemistry within stress-corrosion cracks in alloy steels. *Corros. Sci.* **10**, 839 (1970).
22. Parkins, R., Craig, I. & Congleton, J. Current and potential measurements along simulated cracks. *Corros. Sci.* **24**, 709–730 (1984).
23. Gabetta, G. & Rizzi, R. Electrochemical potentials measured at the tip of a growing fatigue crack in demineralized water 93°C: the effect of frequency, wave form and oxygen content. *Corros. Sci.* **23**, 613617–615620 (1983).
24. Leidheiser, H. & Kissinger, R. O. Y. Chemical analysis of the liquid within a propagating stress corrosion crack in 70:30 brass immersed in concentrated ammonium hydroxide. *Corrosion* **28**, 218–221 (1972).
25. Scott, P., Thorpe, T. & Silvester, D. Rate-determining processes for corrosion fatigue crack growth in ferritic steels in seawater. *Corros. Sci.* **23**, 559–575 (1983).
26. Turnbull, A., Zhou, S. & Hinds, G. Stress corrosion cracking of steam turbine disc steel–– measurement of the crack-tip potential. *Corros. Sci.* **46**, 193–211 (2004).
27. Turnbull, A. The solution composition and electrode potential in pits, crevices and cracks. *Corros. Sci.* **23**, 833–870 (1983).
28. Turnbull, A. Modeling of the chemistry and electrochemistry in cracks—a review. *Corrosion* **57**, 175–189 (2001).
29. Turnbull, A. in *ICF10* (Honolulu 2001, 2013).
30. Turnbull, A. & Psaila-Dombrowski, M. A review of electrochemistry of relevance to environment-assisted cracking in light water reactors. *Corros. Sci.* **33**, 1925–1966 (1992).
31. Turnbull, A. Theoretical analysis of influence of crack dimensions and geometry on mass transport in corrosion–fatigue cracks. *Mater. Sci. Technol.* **1**, 700–710 (1985).

32. Turnbull, A. Theoretical evaluation of the dissolved oxygen concentration in a crevice or crack in a metal in aqueous solution. *Br. Corros. J.* **15**, 162–171 (1980).

33. Cooper, K. R. & Kelly, R. G. in *Materials Solution Conference*. 73–82 (ASM International, 2001).

34. Thomas, S., Sundararajan, G., White, P. D. & Birbilis, N. The effect of absorbed hydrogen on the corrosion of steels: Review, discussion and implications. *CORROSION.* **73**, 426–436 (2017).

35. Hartman, A. On the effect of oxygen and water vapor on the propagation of fatigue cracks in 2024-T3 alclad sheet. *Int. J. Fract. Mech.* **1**, 167–188 (1965).

36. Gangloff, R. P. in *Environment Induced Cracking of Metals* (eds Gangloff, R. P. & Ives, M. B.) 55–109 (NACE, 1989).

37. Gangloff, R. P. in *Fatigue '02* (ed Blom, A.) 3401–3433 (Engineering Materials Advisory Services, 2002).

38. Gangloff, R. P. in *Hydrogen Effects on Material Behavior and Corrosion Deformation Interactions* (eds Moody, N. R., Thompson, A. W., Ricker, R. E., Was, G. W. & Jones, R. H.) 477–497 (TMS-AIME, 2003).

39. Gasem, Z. & Gangloff, R. P. in *Chemisty and Electrochemistry of Corrosion and Stress Corrosion Cracking* (ed Jones, R. H.) 501–521 (TMS-AIME, 2001).

40. Gasem, Z. M. *Frequency Dependent Environmental Fatigue Crack Propagation in the 7XXX Alloy/Aqueous Chloride System*. Ph.D. thesis, Univ. Virginia, (1999).

41. Broom, T. & Nicholson, A. Atmospheric corrosion fatigue of age hardenable aluminum alloys. *J. Inst. Metals* **89**, 183–190 (1960–1961).

42. Wei, R. P. & Gangloff, R. P. in *Fracture Mechanics: Perspectives and Directions, ASTM STP 1020* (eds Wei, R. P. & Gangloff, R. P.) 233–264 (ASTM International, 1989).

43. Wei, R. P. Some aspects of environment-enhanced fatigue-crack growth. *Eng. Fract. Mech.* **1**, 633–651 (1970).

44. Wei, R. P. Fatigue-crack propagation in a high-strength aluminum alloy. *Int. J. Fract. Mech.* **4**, 159–168 (1968).

45. Ro, Y., Agnew, S. R., Bray, G. H. & Gangloff, R. P. Environment-exposure-dependent fatigue crack growth kinetics for Al-Cu-Mg/Li. *Mater. Sci. Eng.: A* **468–470**, 88–97 (2007).

46. Ro, Y. J. *Characterization of exposure dependent fatigue crack growth kinetics and damage mechanisms for aluminum alloys*. Ph.D. thesis, Univ. Virginia, (2008).

47. Ro, Y. J., Agnew, S. R. & Gangloff, R. P. in *Fourth International Very High Cycle Fatigue Conference* (eds Allison, J. E., Wayne J. J., Larsen, J. M. & Ritchie, R. O.) 409–420 (TMS, 2007).

48. Nguyen, T., Brown, B. & Foley, R. On the nature of the occluded cell in the stress corrosion cracking of AA 7075-T651-effect of potential, composition, morphology. *Corrosion* **38**, 319–326 (1982).

49. Cui, Z. Y. et al. Crack growth behavior and crack tip chemistry of X70 pipeline steel in near- neutral pH environment. *Corros. Eng., Sci. Technol.* **51**, 352–357 (2016).

50. Young, L. M., Young, G. A., Scully, J. R. & Gangloff, R. P. in *Light Weight Alloys for Aerospace Applications IV, Proceedings of the "Light Weight Alloys for Aerospace Applications"* Symposium 4th edn (ed Lee E. W.) 3–18 (Minerals, Metals & Materials Society, 1997).

51. Young, L. M. *Microstructural Dependence of Aqueous-Environment Assisted Crack Growth and Hydrogen Uptake in AA 7050*. Ph.D. thesis, Univ. Virginia, (1999).

52. Warner, J. S., Kim, S. & Gangloff, R. P. Molybdate inhibition of environmental fatigue crack propagation in Al-Zn-Mg-Cu. *Int. J. Fatigue.* **31**, 1952–1965 (2009).

53. Warner, J. S. & Gangloff, R. P. Molybdate inhibtion of corrosion fatigue crack propagation in precipitation hardened Al-Cu-Li. *Corros. Sci.* **62**, 11–21 (2012).

54. Gasem, Z. & Gangloff, R. Effect of temper on environmental fatigue crack propagation in 7000-series aluminum alloys. *Mater. Sci. Forum* **331-337**, 1479–1488 (2000).

55. Turnbull, A. & May, A. Steady state electrochemical kinetics of BS 4360 50D structural steel in deaerated 3· 5% NaCl solution of varying pH. *Br. Corros. J.* **22**, 176–181 (1987).

56. Gangloff, R. & Turnbull, A. in *Modeling Environonmental Effects on Crack Growth Processes* (eds Jones, R. H. & Gerberich, W. W.) 55–81 (TMS-AIME, 1985).

57. Crane, C. B., Kelly, R. G. & Gangloff, R. P. Crack chemistry control of intergranular stress corrosion cracking in sensitized Al-Mg. *Corrosion* **72**, 242–263 (2015).

58. Warner, J. S. & Gangloff, R. P. Alloy induced inhibition of fatigue crack growth in age- hardenable Al–Cu Alloys. *Int. J. Fatigue.* **42**, 35–44 (2012).

59. Locke, J. S. Comparison of age-hardenable Al Alloy corrosion fatigue crack growth susceptibility and the effect of testing environment. *Corrosion* **72**, 911–926 (2016).